

Elastic strain at pseudomorphic semiconductor heterojunctions studied by x-ray photoelectron diffraction: Ge/Si(001) and Si/Ge(001)

S. A. Chambers and V. A. Loebs

High Technology Center, Boeing Aerospace & Electronics, Boeing Company, P.O. Box 3999, Seattle, Washington 98124-2499

(Received 10 May 1990)

We have used x-ray photoelectron diffraction to probe strain at the lattice-mismatched semiconductor heterojunctions Ge/Si(001) and Si/Ge(001). Deposition of four-monolayer equivalents of Si on Ge(001) at $\sim 350^\circ\text{C}$ causes cluster formation, whereas deposition of the same amount of Ge on Si(001) at nearly the same temperature results in more laminar growth. These findings are consistent with surface thermodynamic considerations in that Ge has a lower surface free energy than does Si. Careful measurement of the polar angle at which the forward-scattering-induced diffraction peak along [011] occurs provides an estimate of the perpendicular lattice constant a_\perp . By this means, we estimate a_\perp to be 5.62 and 5.31 Å for the Ge/Si(001) and Si/Ge(001) interfaces, respectively. In order to obtain a more quantitative measure of the strain, we have used reliability (R) factor analysis to determine a_\perp by comparison of experiment with single-scattering calculations. This analysis yields values of 5.75 ± 0.04 and 5.38 ± 0.08 Å for Ge/Si and Si/Ge, respectively. These values suggest less distortion by ~ 0.1 Å in the strained overlayers than what is predicted by classical elastic theory. However, agreement with the strain predicted for the Ge/Si(001) interface by more accurate total-energy pseudopotential calculations is excellent. Finally, high-angular-resolution azimuthal scans at any polar angle are not particularly sensitive to tetragonal distortion, at least for the diamond crystal structure.

INTRODUCTION

Strain effects at lattice-mismatched semiconductor heterojunctions cause major perturbations to the electronic structure of the system. Tetragonal distortion associated with pseudomorphic growth can result in large changes in the valence- and conduction-band electronic structure of the strained epilayer as well as changes in the interface band offset.¹⁻³ These perturbations can be used to one's advantage in device applications. For instance, recent calculations suggest that new optical transitions of some direct or quasidirect character arise through zone-edge and zone-center mixing in strained-layer Si/Ge superlattices.⁴⁻⁷ Therefore, the ability to control and measure strain represents a significant technological advantage in advanced electronic-device design and processing. In this paper we address the issue of strain measurement. It has been shown that high-resolution x-ray diffraction is a powerful probe of strain in superlattices.^{8,9} However, direct strain determination in *single* pseudomorphic epilayers is much more difficult to carry out with x-ray diffraction, largely due to an overwhelming signal contribution from the substrate. Glancing-incidence x-ray diffraction has recently been shown to be useful in determining the in-plane strain.¹⁰ By carefully selecting the diffraction conditions, one can minimize thermal diffuse scattering from the bulk and thereby increase the sensitivity to strain relief on the top tens of angstroms of the material. However, it is in general not possible to distinguish between strain relief and intermixing with this technique. Intermixing can readily occur at the temperatures required to obtain high-quality crystalline epilayers.

Standing-wave x-ray diffraction at glancing angles of incidence is, in principle, a useful method of probing strain perpendicular to the interface. In this technique the antinodes of the standing wave can be positioned at various depths below the surface by tuning the photon energy. Auger and fluorescence emission from atoms in the strained overlayer are expected to maximize when the depths of the antinodes coincide with the z coordinates of atoms in the strained overlayer. An investigation of this sort has been carried out for $\text{CoSi}_2/\text{Si}(111)$.¹¹

It has recently been shown that high-energy x-ray photoelectron diffraction (XPD) can be used to directly determine strain at a lattice-mismatched heterojunction by accurately measuring $\theta_{[011]}$, the polar angle at which the forward-scattering-induced diffraction peak along [011] falls.¹² Moreover, the atom specificity of the technique permits one to distinguish between strain relief and intermixing. Determination of the perpendicular lattice constant a_\perp for four monolayers (ML) of nonintermixed, pseudomorphic Si on Ge(001) was carried out by two means. The first of these involved a simple computation of a_\perp from the relation $a_\perp = a_\parallel \tan \theta_{[011]}$. The second method involved employing single-scattering theory to calculate the portion of the angular distribution which includes the [011] diffraction peak as a function of a_\perp , and then carry out a reliability (R)-factor analysis. These two methods led to a_\perp values of 5.31 ± 0.04 and 5.34 ± 0.04 Å, respectively. Although well within experimental error of one another, these values are somewhat in excess of that predicted by elastic theory, 5.26 Å.

In this paper we describe the more complete set of the experiments summarized in Ref. 12 as well as an analo-

gous investigation of the inverted interface—Ge/Si(001). In summary, we have found that (i) four-monolayer equivalents (ML-EQ) of Si grow as clusters, whereas the same deposition of Ge on Si(001) grows in a more laminar fashion, (ii) the value of a_{\perp} suggested by the position of the [011] diffraction peak should, in general, be taken only as an estimate, (iii) a_{\perp} is best determined by comparison with quantum-mechanical scattering calculations in which the strain is systematically varied and compared with experiment by means of R -factor analysis, and (iv) the values of a_{\perp} determined by the present investigation indicate less strain by $\sim 0.1 \text{ \AA}$ for both tension and compression than what is predicted by elastic theory, but are in good agreement with values predicted by total-energy calculations, at least for the Ge/Si(001) case.

EXPERIMENT

All experiments were carried out in a custom-built system which combines molecular-beam-epitaxy (MBE) growth of metals and semiconductors with x-ray photoelectron diffraction (XPD), low-energy electron diffraction (LEED), and x-ray photoelectron spectroscopy (XPS). The XPS system consists of a Surface Science Instruments Series 300 x-ray photoelectron spectrometer equipped with a monochromatic Al $K\alpha$ x-ray source, hemispherical analyzer, multichannel detector, and externally actuated apertures to permit angle-resolved measurements. A precision ($\pm 0.1^{\circ}$) two-axis sample manipulator in conjunction with the aforementioned apertures permits XPD experiments to be carried out in a scanned-angle mode. Both polar- and azimuthal-angle intensity distributions of Si $2p$ photoemission were measured with a half-angle of acceptance ($\Delta\theta_{1/2}$ and $\Delta\phi_{1/2}$) of 3.3° and compared with angular distributions calculated by means of plane-wave single-scattering theory.¹³ R -factor analysis was performed to assess more accurately the level of agreement between theory and experiment. Here we define the reliability factor as

$$R(n) = \sum_{\mathbf{k}} \text{abs}[I_{\text{obs}}(\mathbf{k}) - nI_{\text{calc}}(\mathbf{k})] / \sum_{\mathbf{k}} I_{\text{obs}}(\mathbf{k}),$$

where $I_{\text{obs}}(\mathbf{k})$ and $I_{\text{calc}}(\mathbf{k})$ are measured and calculated photoelectron intensities along wave vector \mathbf{k} , and n is a normalization constant for equating theoretical with experimental intensities. For a given angular scan, a search for the value of n that minimizes $R(n)$ was carried out for each geometry tested.

Ge(001) substrates were generated by growing several hundred angstroms of Ge at $\sim 330^{\circ}\text{C}$ on GaAs(001) substrates, which were, in turn, prepared in a Perkin-Elmer model 430 MBE system. GaAs surface preparation consisted of a standard degrease and acid etch, followed by growth of a $1\text{-}\mu\text{m}$ -thick GaAs buffer layer and an As cap in the Perkin-Elmer MBE chamber. As-capped samples were then transferred through air to the Si/Ge MBE chamber, where the As cap was desorbed by flashing briefly to $\sim 415^{\circ}\text{C}$. After Ge-epilayer growth, the surfaces exhibited clear, sharp orthogonal $p(2\times 1)$ LEED patterns. Although in possession of some density of single steps as judged by the two $p(2\times 1)$ domains, surfaces

prepared in this way should have a much lower density of vacancy defects than bulk Ge(001) specimens that are sputtered and annealed at high temperature.

Si(001) substrates were prepared by performing a liquid degrease, acid etch, and ultrahigh-vacuum (UHV) anneal to $\sim 900^{\circ}\text{C}$ while exposed to a low Si flux. The latter step has been found to significantly enhance SiO_2 desorption at a relatively low temperature of 900°C through the process of Si-beam-induced decomposition of SiO_2 .¹⁴ This procedure resulted in clean surfaces which exhibited clear, sharp orthogonal $p(2\times 1)$ LEED patterns.

Four ML-EQ of Si or Ge, as measured by a quartz-crystal oscillator, were grown at substrate temperatures of $330\text{--}390^{\circ}\text{C}$. This range of temperature was chosen because it is above that required to achieve good epitaxy, but below the temperature at which intermixing occurs.¹² Sharp, clear orthogonal $p(2\times 1)$ LEED patterns which were virtually identical to those of the substrates remained after Si and Ge overlayer growth.

RESULTS

We show in Fig. 1 a schematic diagram of our XPD spectrometer geometry (inset), the diamond crystal structure, and the coordinate system we have used to orient the specimen with respect to the spectrometer. We will refer to this diagram often to aid in understanding the significance of the results.

In Fig. 2 we show measured and calculated XPD polar scans in the (010) azimuth of thin epitaxial films of Ge on Si(001), Si(001), and thin epitaxial films on Si on Ge(001). Integrated intensities after Shirley background subtraction are plotted in 1.0° increments from $\theta = 14^{\circ}$ to 98° .

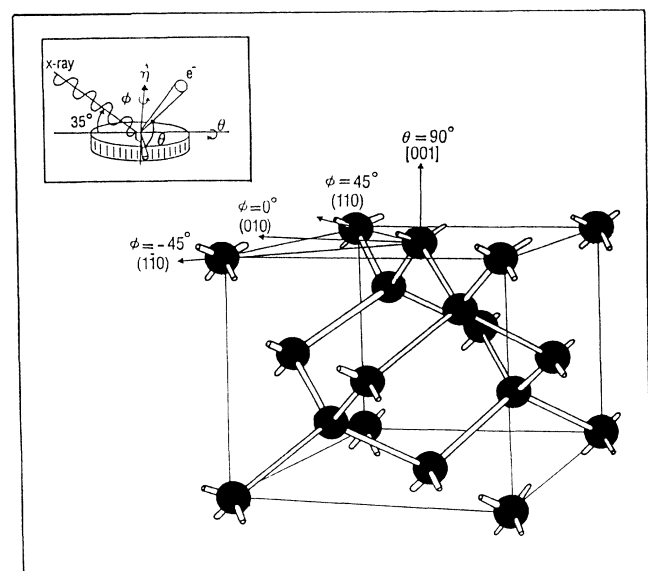


FIG. 1. Diamond crystal structure and coordinate-system orientation used in the present work, along with a schematic representation of sample-diffractometer geometry (inset).

The substrate emission peak along the surface normal ($\theta=90^\circ$) was used as an internal calibration of the goniometer-analyzer geometry. In this way, other diffraction peaks could be measured with an accuracy of $\pm 0.2^\circ$. Looking first at the data for Si(001), major forward-scattering-induced peaks are seen at $\theta=45^\circ$ and 90° . These peaks result from scattering and constructive interference along the [011] and [001] low-index directions, respectively. Additional structures of a more complex origin involving interference of many scattered-wave portions along with the unscattered-wave portion are also seen between 60° and 80° , and below 30° . Examination of the diamond crystal structure (Fig. 1) reveals that the peaks along [011] and [001] are not expected until epitaxial films have achieved thickness of 3 and 5 ML, respectively. At these coverages, photoelectrons generated in the first monolayer can forward-scatter from atoms in the third monolayer at 45° and in the fifth monolayer at 90° .^{15,16}

When 4 ML-EQ of Ge are grown on Si(001) at 390°C , the only peak observed falls slightly above $\theta=45^\circ$. The absence of a peak at $\theta=90^\circ$ indicates that the layer has

grown in a nearly laminar fashion. Clustering in which fifth- (or higher-) layer formation occurs would give rise to a peak along the surface normal, as discussed above, and as can be seen by examination of the theory curves for 4- and 5-ML epitaxial films shown in Fig. 2. A weak peak is predicted to develop along [001] when a fifth layer is present. Values of 5.75 and 5.43 Å were assumed in the calculations for a_\perp and a_\parallel , respectively. This choice of parameters will become apparent shortly. Interestingly, the calculated peak along [001] was observed to flatten as tetragonal distortion in the overlayer was increased, indicating that structurally sensitive interference effects in addition to simple forward scattering can have a significant effect on the shapes of peaks along low-index directions. Although the calculated peak intensity along the surface normal associated with growth of the fifth layer is weak, previous experimental measurements¹⁶ as well as those shown in Fig. 5 for Ge/GaAs(001) show that this peak is substantial once growth of the fifth layer occurs. Therefore, the virtual absence of a peak in the present data demonstrates that laminar growth has occurred. Indeed, laminar growth of Ge on Si(001) is expected on thermodynamic grounds because the surface free energy of Ge is less than that of Si.¹⁷

Looking now at the data for 4 ML-EQ Si on Ge(001) grown at 330°C , we notice strong peaks along both [011] and [001], indicating that at least partial fifth-layer formation has occurred. Fifth-layer formation is confirmed by examining single-scattering calculations for 4 and 5 ML epitaxial films of Si on Ge(001), which again show that the onset of the peak along [001] indeed coincides with growth of the fifth layer. These calculations, which were carried out for $a_\perp=5.34$ Å and $a_\parallel=5.65$ Å, are shown adjacent to the experimental angular distribution in the bottom half of Fig. 2. (This choice of lattice constants will become obvious shortly.) It is tempting to try to extract the extent of fifth-layer formation from the relative intensities of the [011] and [001] diffraction peaks by comparison with theory. However, it is well known that multiple scattering along chains of two or more atoms causes defocusing that effectively reduces the intensity of the associated forward-scattering peaks compared to analogous single-scattering calculations.¹⁸⁻²⁰ Therefore, such an analysis is not expected to yield accurate results unless multiple scattering is included. However, there is no question that a 4 ML-EQ deposit of Si on Ge(001) results in cluster formation in which the clusters are at least five layers deep. Island formation (Volmer-Weber growth) is expected on the basis of the fact that Ge possesses a lower surface free energy than does Si.¹⁷

Tetragonal distortion in the epitaxial film can be determined by analyzing the position of the [011] peak. As seen at the top of Fig. 2, tensile expansion in the plane of the interface, as would occur for pseudomorphic growth of Si on Ge(001), will result in compression in the direction normal to the interface. Any such compression is expected to result in a shift to lower polar angle in the [011] diffraction peak. Similarly, an upward shift in polar angle is expected and observed for growth of Ge on Si(001). These shifts can be used to estimate a_\perp , as described below.

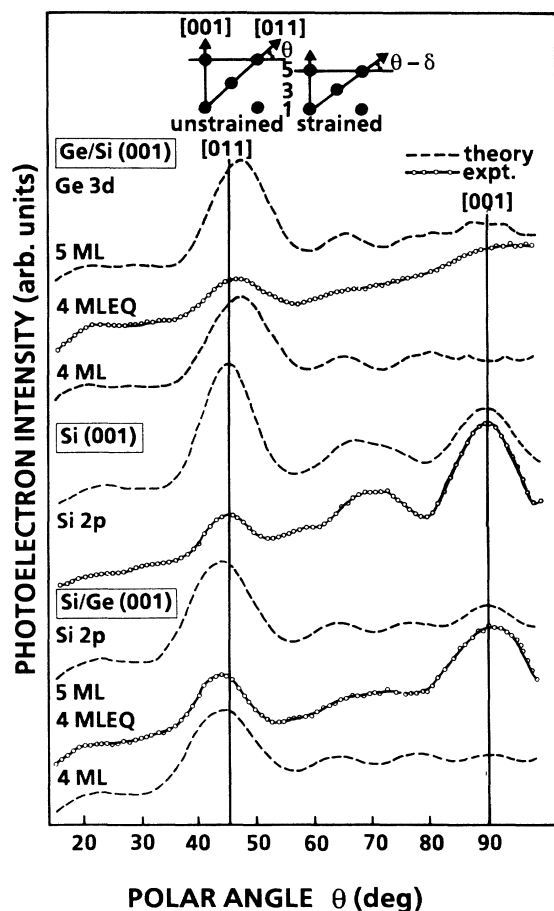


FIG. 2. Measured and calculated polar-angle scans in the (010) azimuth for Ge/Si(001), Si(001), and Si/Ge(001).

We show in Fig. 3 polar-angle scans for Ge/Si(001), Si(001), and Si/Ge(001) in which the [011] forward-scattering peak has been plotted in expanded form after a linear background subtraction. Precise angular calibration based on alignment of the [001] diffraction peak associated with substrate emission at $\theta=90.0^\circ$ was carried out in order to ensure high accuracy and precision in the position of the [011] peak. Also shown are calculated forward-scattering peaks which give optimal agreement with experiment as judged by R -factor analysis (to be discussed below).

Looking first at the scan for Si(001)- 2×1 , we note that the Si 2p [011] forward-scattering peak is highly symmetric and falls at $44.9^\circ \pm 0.2^\circ$, which is within experimental error of the expected value of 45.0° for a fcc lattice that is unstrained except for the surface reconstruction. The presence of orthogonal $p(2\times 1)$ domains has no measurable effect on the angle at which the peak is observed. The full width at half-maximum (FWHM) of the substrate diffraction feature is 8.2° . The [011] peaks for strained Ge on Si(001) and strained Si on Ge(001) fall at $46.0^\circ \pm 0.2^\circ$ and $43.2^\circ \pm 0.2^\circ$, respectively. Using the simple relation $a_\perp = a_\parallel \tan\theta_{[011]}$, a_\perp is estimated to be $5.62 \pm 0.04 \text{ \AA}$ and $5.31 \pm 0.04 \text{ \AA}$ for Ge/Si and Si/Ge, respectively. The uncertainty of $\pm 0.04 \text{ \AA}$ in a_\perp is a direct result of the $\pm 0.2^\circ$ uncertainty in the angle at which the [011] peak

falls. We assume that the strained overlayers are commensurate with the substrate. This assumption is consistent with the lack of visible position change of the integral-order LEED spots or pattern degradation upon growth of the Si and Ge overlayers. It is also consistent with recent glancing-incidence x-ray-diffraction results which show no change in the in-plane lattice constant until the onset of strain relaxation.¹⁰ Thus, a_\parallel for the overlayer is same as that for the substrate— 5.43 \AA for Si(001) and 5.65 \AA for Ge(001). The FWHM values are 10.5° and 9.3° for the Ge 3d and Si 2p peaks, respectively. We will comment on this difference in peak width below, but it is first instructive to consider an alternate way of determining a_\perp —namely comparison of the experimental angular distributions with those calculated by means of plane-wave single-scattering theory.

We show in Fig. 4 an R -factor analysis of the angular distributions for the strained overlayers in Fig. 3. Some striking differences are seen. First, the R -factor curve for Ge/Si exhibits a sharper minimum than does the curve for Si/Ge. Second, the value of the R factor is lower by a factor of 3 at the minimum of the Ge/Si curve than that for the Si/Ge curve. These differences are closely related to the difference in peak width, which ultimately arises from multiple-scattering effects. The fact that Si on Ge(001) clusters to a thickness of at least 5 ML means that photoelectrons emitted from the first layer will in actuality undergo at least double forward scattering along

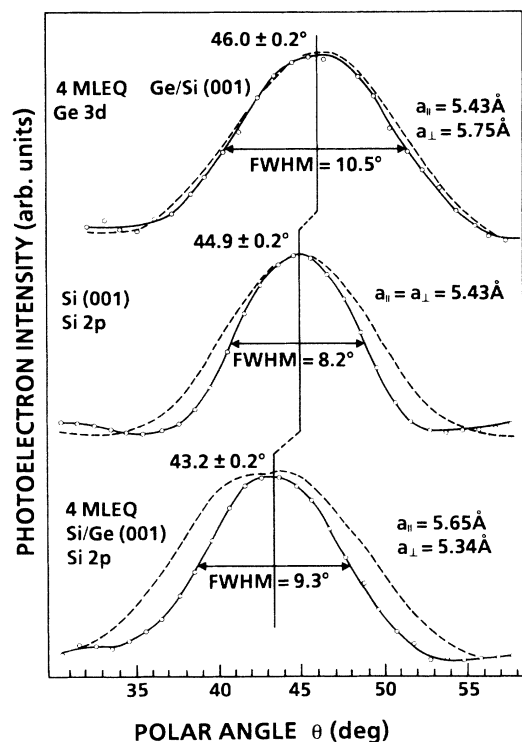


FIG. 3. Measured and calculated [011] forward-scattering peaks after linear background subtraction for 4 ML-EQ Ge/Si(001), Si(001), and 4 ML-EQ Si/Ge(001). The value of a_\perp used in the calculations for the strained overlayers is the one that yields the minimum R factor (Fig. 4).

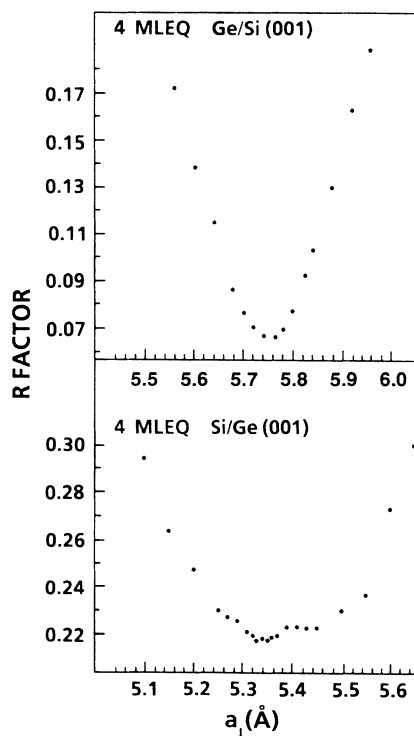


FIG. 4. R factor vs a_\perp for 4 ML-EQ Ge/Si(001) and (4 ML-EQ Si/Ge(001)).

[011]. Multiple forward scattering has been predicted to cause a defocusing and narrowing of the diffraction peak,^{19–21} and in Fig. 5 we show direct experimental evidence for this prediction.

Plotted in Fig. 5 are complete (bottom panel) and expanded, partial (top panel) polar-angle distributions for 4 and 5 ML-EQ Ge on GaAs(001) grown at 350°C. This system was chosen to illustrate the broadening effect of multiple scattering because it is 99.876% lattice matched. Thus, additional broadening mechanisms such as partial film relaxation at or above the critical thickness will not come into play. The presence of a weak peak along the surface normal at 4 ML demonstrates that partial fifth-layer formation has occurred. Thus, the [011] low-index direction in the overlayer consists of two (three) atoms where the film is four (five) layers deep. It is then expected that the [011] forward-scattering peak should be somewhat narrower than that for 4 ML-EQ Ge on Si(001), for which little or no fifth-layer formation occurs. Indeed, the peak width is 9.6°, which is $\sim 1^\circ$ less than the value measured for Ge/Si(001). However, growth of 5 ML-EQ of Ge on GaAs(001) results in completion of the fifth layer and perhaps initiation of the sixth (or higher) layer. Thus, multiple scattering of *all* photoelectrons emitted in the first layer occurs along [011]. As a result, the Ge 3d diffraction peak along [011] undergoes $\sim 1^\circ$ of additional narrowing. This narrowing effect with additional atoms

in the chain is not reflected in our calculations because of the neglect of multiple scattering. Thus, the calculated peak width for the Si/Ge(001) interface (in which significant multiple scattering occurs along [011] in the overlayer) is larger by a few degrees than the experimental counterpart. This reality leads to a relatively poor level agreement between theory and experiment (Figs. 3 and 4). In contrast, Ge grows in a laminar fashion on Si(001). Therefore, only single-scattering events occur, and the experimental and theoretical peak widths are very nearly the same. A much better fit with theory is achieved as a result.

Returning to Fig. 4, values of a_\perp are readily extracted from the R -factor curves. There is no ambiguity in the case of Ge/Si(001); a symmetric minimum occurs at $5.75 \pm 0.04 \text{ \AA}$. The situation is complicated for the Si/Ge(001) system by the large difference in peak width between theory and experiment. This reality causes the R -factor curve to be broader and show some discontinuous structure near the minimum. The absolute minimum occurs at $5.34 \pm 0.04 \text{ \AA}$. There is maximum overlap in the theoretical and experimental peak positions at this value of a_\perp . However, there is also a flat portion of the curve from 5.39 to 5.45 Å for which the R factor is very close to the absolute minimum. The presence of this plateau compels us to conclude that the most reasonable value of a_\perp that can be extracted from the R -factor curve is

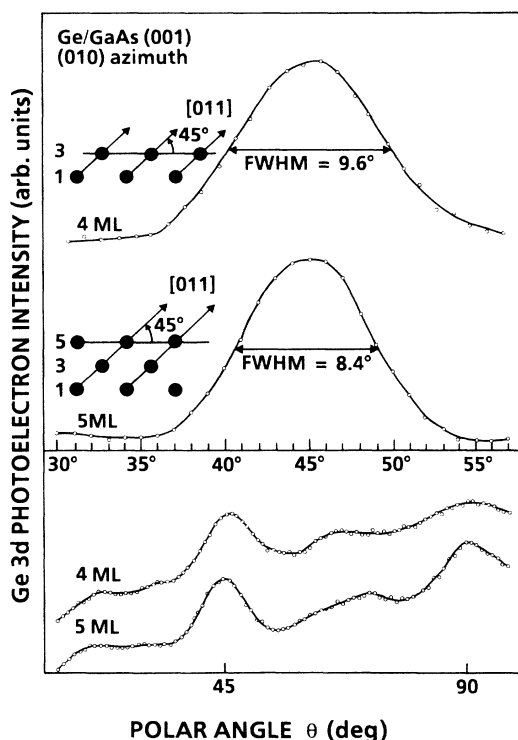


FIG. 5. Full polar angular distributions in the (010) azimuth for 4 and 5 ML-EQ Ge/GaAs(001) (bottom panel), and expanded plots of the [011] peak for the same interfaces after a linear background subtraction (top panel).

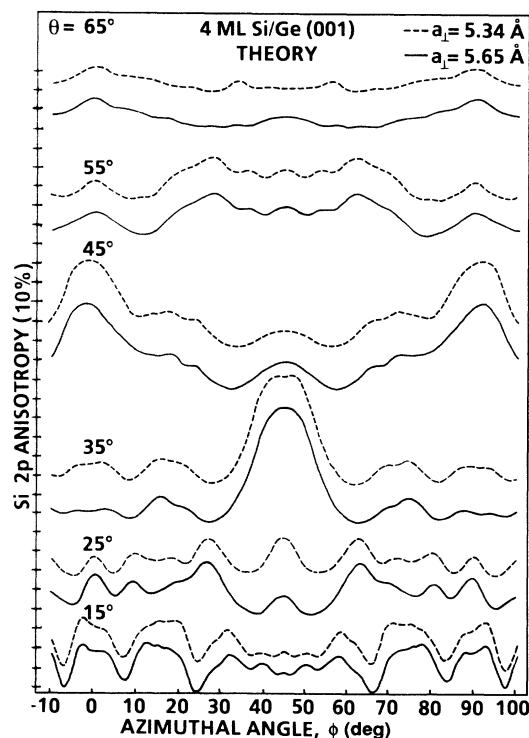


FIG. 6. Calculated azimuthal angle distributions for 4 ML Si/Ge(001) at various polar angles in which different values of a_\perp have been assumed. The lack of sensitivity of the structure in these angular distributions to a_\perp is evident.

5.38 ± 0.08 Å. This value, though not at the absolute minimum, is at the center of the bottom of the curve. Furthermore, an uncertainty of ± 0.08 Å covers the entire region in the vicinity of the minimum for which the first derivative of the R -factor curve is approximately zero.

It is also of interest to investigate the sensitivity of high-angular-resolution azimuthal-angle distributions to tetragonal distortion in the epilayer. We present in Fig. 6 calculated azimuthal-angle distributions at several polar angles for 4 ML Si/Ge(001) in which we assume two widely divergent values of a_{\perp} . The values of a_{\perp} are 5.34 Å, the value deduced from the absolute minimum in Fig. 4, and 5.65 Å, which corresponds to an overlayer with perfect cubic symmetry. The angular averaging used in the calculations corresponds to that of the smaller of our two apertures— $\Delta\theta_{1/2} = \Delta\phi_{1/2} = 1.7^{\circ}$. The calculation runs from the (010) azimuthal plane ($\phi = 0^{\circ}$) to the (100) plane ($\phi = 90^{\circ}$) (see Fig. 1). Inspection of Fig. 5 reveals that the level of sensitivity of such angular scans to a_{\perp} is not particularly high. Angular distributions for the two values of a_{\perp} are very similar for $\theta = 65^{\circ}, 55^{\circ}, 45^{\circ}, 35^{\circ}$, and 15° , and determination of a_{\perp} from a comparison with experiment would not be feasible. There is, however, some degree of sensitivity available from the scan at $\theta = 25^{\circ}$. There is a large change in relative intensity of the feature at $\phi = 45^{\circ}$ compared to those at 27° and 63° over the chosen range of a_{\perp} . However, the relative intensities of these three features are not a sensitive function of a_{\perp} over this range of values. Therefore, we conclude that polar scans over [011] are a more sensitive probe of tetragonal distortion than azimuthal scans at higher angular resolution, at least for the diamond crystal structure.

DISCUSSION

There are to our knowledge no other experimental determinations of a_{\perp} for single layers of thin, pseudomorphic Si on Ge(001) or Ge on Si(001) reported in the literature. However, Pearsall *et al.* have recently reported transmission-electron-microscopy (TEM) and electroreflectance measurements on Si/Ge superlattices in which each layer was 4 ML-EQ thick.²² Analysis of TEM lattice images indicates that interface roughness of the order of ± 1 ML existed in the superlattice. This observation is consistent with our conclusions about fifth-layer formation during the deposition of the Si layer. They also note that large differences exist between calculated and measured optical matrix elements for structurally induced electronic states near the indirect gap of the superlattice. These matrix elements depend critically on atomic coordinates, and elastic theory is typically used to determine the perpendicular strain in the absence of experimental input. Therefore, the observed discrepancies may be a result of the deviation between the present determination of a_{\perp} and that calculated by elastic theory.

Classical elastic theory has frequently been used to estimate the tetragonal distortion associated with lattice mismatch. The calculation starts with experimental values of elastic stiffness constants for the bulk material, as determined by elastic wave velocity measurements. These constants are then related to the strain tensor

through the classical stress-strain relationship. Matrix rotations then permit one to obtain the strain normal to the interface (ϵ_{33}) in terms of ratios of stiffness constants.²³ The perpendicular lattice constant is then given by the relation $a_{\perp} = (1 + \epsilon_{33})a$, where a is the bulk lattice constant. Application of this equation to the Si/Ge(001) and Ge/Si(001) interfaces yields a_{\perp} values of 5.26 Å and 5.82 Å, respectively. These values suggest ~ 0.1 Å more strain than what we have determined by XPD. The discrepancy may originate in the classical nature of the calculation and/or the use of bulk elastic constants in an interfacial calculation. A similar departure from elastic theory has also been suggested by ion scattering for the Si/Ge/Si(001) system, in which a_{\perp} was estimated by comparing simulations of the ion angular intensity profiles with experiment.²⁴

In contrast, agreement of the present experimental results for Ge/Si(001) with the predictions from a recent total-energy pseudopotential calculation is quite good.²⁵ In this calculation, a_{\perp} values for both Si and Ge epilayers in a Si_4Ge_4 superlattice on Si(001) were determined by total-energy minimization. All strain was predicted to be taken up by the Ge layers, and a_{\perp} was predicted to be 5.72 Å. Agreement with the present experimental value of 5.75 ± 0.04 Å is excellent.

The analysis of the Ge/Si(001) data (Figs. 3 and 4) suggests that, in general, determination of a_{\perp} simply by means of measurement of $\theta_{[011]}$ may lead only to an approximate value. The peak position suggests a value of 5.62 Å for Ge/Si(001). In contrast, R -factor analysis of the polar angular intensity distribution over the [011] peak yields a value of 5.75 Å. The origin of this discrepancy can be seen by careful inspection of the upper panel of Fig. 3. The experimental peak maximum falls at a slightly lower polar angle than the calculated peak maximum at the value of a_{\perp} that minimizes the R factor (5.75 Å). However, the overall deviation between theory and experiment is minimized at 5.75 Å. The situation is complicated by the presence of multiple scattering in the experimental data for the Si/Ge(001) system. Here the uncertainty in the R -factor analysis is large enough that the a_{\perp} values derived from the simple trigonometric calculation and the more involved R -factor analysis are within the estimated uncertainties.

Closely related to the issue raised in the preceding paragraph is the question of spherical wave effects in single-scattering calculations. It is thought that the so-called "small-atom approximation," which amounts to assuming that the outgoing photoelectron wave can be taken to be a plane wave over the dimensions of the scattering potential, incurs some error at nearest-neighbor distances. It has been found that spherical-wave effects reduce scattering amplitudes relative to plane-wave values, but do not cause changes in the phase shifts at high kinetic energies (~ 950 eV).²⁶ Moreover, this effect is observed only for scattering angles of $\lesssim 30^{\circ}$, which includes the forward-scattering regime upon which the present analysis is based. We have performed calculations which implicitly include spherical-wave effects using a high-energy approximation by Rehr *et al.* which is

readily included in a single-scattering formalism.²⁷ We have found that inclusion of such effects in the calculation of the [011] forward-scattering peak produces virtually no change in either the peak shape or the R -factor analysis relative to the plane-wave results. The most probable reason for this insensitivity is the fact that interaction with the outer portion of the scattering potential (where wave curvature is most likely to affect the scattering) is negligible at the kinetic energies employed (~ 1400 eV). On the basis of this result, we conclude that the small-atom approximation is completely valid at high kinetic energies for all scattering events, including those involving nearest neighbors.

In addition to multiple scattering, partial film relaxation at or above the critical thickness is also expected to result in broadening of the [011] peak. However, a large peak asymmetry will accompany such broadening if this phenomenon occurs. The physical cause for this broadening and asymmetry is simply that a partially relaxed film does not possess a unique value of a_{\perp} . Portions of the film remain unrelaxed, while other portions undergo partial relaxation.¹⁰ Thus, the measured [011] scattering peak is actually the sum of two (or more) peaks originating in different portions of the film. If the film is locally five or more layers deep, multiple scattering will occur, and the individual scattering peaks will be rather narrow. The sum of these peaks will be broad, asymmetric (provided portions of the film with different a_{\perp} values are not present in equal amounts), and will, upon analysis, yield an *average* value of a_{\perp} over a macroscopic region of the film. We have observed this phenomenon for Si/Ge(001), and the peak asymmetry in combination with the larger value of a_{\perp} relative to the fully strained case makes broadening by partial film relaxation rather easy to distinguish from broadening by multiple scattering.

The present work suggests that forward-scattering peaks are more sensitive to tetragonal distortion than diffraction fine structure away from low-index directions.

However, this conclusion appears to be strongly dependent on the crystal structure being investigated. Fadley has demonstrated a high degree of sensitivity to tetragonal distortion in the NiO/Ni(001) system by means of high-angular-resolution azimuthal scans at $\theta=45^{\circ}$.²⁸ The intensities of symmetry-relaxed diffraction peaks away from [101] and [011] were found to be strongly dependent on the ratio of a_{\perp} to a_{\parallel} . The fact that such sensitivity is not observed with the diamond structure at a similar level of angular resolution suggests that this kind of sensitivity is crystal-structure dependent.

CONCLUSIONS

We have used x-ray-photoelectron diffraction to probe strain at the lattice-mismatched semiconductor heterojunctions Ge/Si(001) and Si/Ge(001). Careful measurement of the polar angle at which the forward-scattering-induced diffraction peak along [011] occurs provides a reasonable estimate of the perpendicular lattice constant a_{\perp} . By this means, we have measured a_{\perp} in the fully strained Ge and Si overlayers to be 5.62 ± 0.04 and 5.31 ± 0.04 Å, respectively. In addition, we have used R -factor analysis to determine a_{\perp} by comparison with single-scattering calculations. This analysis yields values of 5.75 ± 0.04 and 5.38 ± 0.08 Å, in reasonable agreement with the simple geometric method. These values suggest that the overlayers are less strained than what is predicted by classical elastic theory by ~ 0.1 Å. However, the strain measured by XPD is in very good agreement with what has been predicted by means of total-energy pseudopotential calculations, at least for the Ge/Si(001) case. We have also attempted to determine a_{\perp} from high-angular-resolution azimuthal scans away from low-index directions. However, these measurements do not possess the same degree of sensitivity as the polar-scan measurements, at least for the diamond crystal structure.

¹E. P. O'Reilly, *Semicond. Sci. Technol.* **4**, 121 (1989), and references therein.

²T. P. Pearsall, F. H. Pollak, J. C. Bean, and R. H. Hull, *Phys. Rev. B* **33**, 6821 (1986).

³G. P. Schwartz, M. S. Hybertsen, J. Bevk, R. G. Nuzzo, J. P. Mannaerts, and G. J. Gualtieri, *Phys. Rev. B* **39**, 1235 (1989).

⁴S. Froyen, S. M. Wood, and A. Zunger, *Phys. Rev. B* **36**, 4574 (1987).

⁵C. Ciraci and I. P. Batra, *Phys. Rev. Lett.* **58**, 2114 (1987).

⁶M. S. Hybertsen and M. Schlüter, *Phys. Rev. B* **36**, 9683 (1987).

⁷S. Satpathy, R. M. Martin, and C. G. Van de Walle, *Phys. Rev. B* **38**, 13 237 (1988).

⁸J. C. Bean, L. C. Feldman, A. T. Fiory, S. Hakahara, and I. K. Robinson, *J. Vac. Sci. Technol. A* **2**, 4365 (1984).

⁹P. J. Orders and B. F. Usher, *Appl. Phys. Lett.* **50**, 980 (1987).

¹⁰J. E. MacDonald, A. A. Williams, R. van Silfout, J. F. van der Veen, M. S. Finney, A. D. Johnson, and C. Norris (unpublished).

¹¹A. E. M. J. Fischer, E. Vlieg, J. F. van der Veen, M. Clausnitzer, and G. Materlik, *Phys. Rev. B* **36**, 4769 (1987).

¹²S. A. Chambers and V. A. Loebis, *Phys. Rev. Lett.* **63**, 640 (1989).

¹³C. S. Fadley, in *Progress in Surface Science*, edited by S. G. Davison (Pergamon, New York, 1984), Vol. 16 (3), pp. 327–365.

¹⁴D. C. Streit and F. G. Allen, *J. Appl. Phys.* **61**, 2894 (1987).

¹⁵S. A. Chambers and T. J. Irwin, *Phys. Rev. B* **38**, 7484 (1988).

¹⁶S. A. Chambers, *J. Vac. Sci. Technol. A* **7**, 2459 (1989).

¹⁷L. Z. Mezey and J. Giber, *Jpn. J. Appl. Phys. Pt. 1* **21**, 1569 (1982).

¹⁸S. Y. Tong, H. C. Poon, and D. R. Snider, *Phys. Rev. B* **32**, 2096 (1985).

¹⁹M.-L. Xu, J. J. Barton, and M. A. Van Hove, *Phys. Rev. B* **39**, 8275 (1989).

²⁰M.-L. Xu and M. A. Van Hove, *Surf. Sci.* **207**, 215 (1989).

²¹A. P. Kaduwela, G. S. Herman, D. J. Friedman, C. S. Fadley, and J. J. Rehr, *Phys. Scr.* (to be published).

²²T. P. Pearsall, J. Bevk, J. C. Bean, J. Bonar, and J. P. Mannaerts, *Phys. Rev. B* **39**, 3741 (1989).

²³R. W. Vook and F. Witt, *J. Appl. Phys.* **36**, 2169 (1965).

²⁴L. C. Feldman, J. Bevk, B. A. Davidson, H.-J. Gossmann, and J. P. Mannaerts, *Phys. Rev. Lett.* **59**, 664 (1987).

²⁵S. Froyen, D. M. Wood, and A. Zunger, *Phys. Rev. B* **37**, 6893 (1988).

²⁶J. Mustre de Leon, J. J. Rehr, C. R. Natoli, C. S. Fadley, and

J. Osterwalder, *Phys. Rev. B* **39**, 5632 (1989).

²⁷J. J. Rehr, R. C. Albers, C. R. Natoli, and E. A. Stern, *Phys. Rev. B* **34**, 4350 (1986).

²⁸C. S. Fadley, *Phys. Scr.* **T17**, 39 (1987).